Model-Based Fault Diagnosis in Electric Drives Using Machine Learning

Yi Lu Murphey, *Senior Member, IEEE*, M. Abul Masrur, *Senior Member, IEEE*, ZhiHang Chen, and Baifang Zhang

***Abstract*—Electric motor and power electronics-based inverter are the major components in industrial and automotive electric drives. In this paper, we present a model-based fault diagnostics system developed using a machine learning technology for detecting and locating multiple classes of faults in an electric drive. Power electronics inverter can be considered to be the weakest link in such a system from hardware failure point of view; hence, this work is focused on detecting faults and finding which switches in the inverter cause the faults. A simulation model has been developed based on the theoretical foundations of electric drives to simulate the normal condition, all single-switch and post-short-circuit faults. A machine learning algorithm has been developed to automatically select a set of representative operating points in the (torque, speed) domain, which in turn is sent to the simulated electric drive model to generate signals for the training of a diagnostic neural network, fault diagnostic neural network (FDNN). We validated the capability of the FDNN on data generated by an experimental bench setup. Our research demonstrates that with a robust machine learning approach, a diagnostic system can be trained based on a simulated electric drive model, which can lead to a correct classification of faults over a wide operating domain.**

***Index Terms*—Electric drives, electric vehicle, field-oriented control (FOC), fuzzy techniques, hybrid vehicle, inverter, machine learning, model-based diagnostics, motor, neural network, power electronics.**

I. Introduction

THREE-PHASE induction motors using techniques such as the field-oriented control (FOC) [1]–[7] to provide precise torque are widely used in various industrial applications, including the automotive power train for electric and hybrid vehicles. The control in these drives is realized by solid-state electronic switches (e.g., IGBT, MOSFET, etc.) being turned on or off [8]. In response to a control algorithm, a reference voltage is generated, and the inverter synthesizes this voltage reference command using techniques such as pulse-width modulation (PWM) or space-vector modulation (SVM) [4]. If a switch fails to function in the way it was intended to, the voltage synthesis process will be impaired, leading to failure in getting proper voltage at the motor terminals, and hence, failure in obtaining the requisite torque at the motor shaft. Failure of the switches can take place in the form of "open" and "short" circuits, as well as failure of reverse diodes in the switches.

Although a motor is relatively a more robust device compared to an inverter, motor windings can deteriorate with time, which can result in either open or shorted windings, fully or partially. When this happens, the motor will fail to generate proper shaft torque or any torque at all, in spite of the fact that the inverter is applying proper voltage input to the motor. Hence, the electric drive can malfunction due to the fault of either the inverter or the motor. However, the inverter is considered to be the weakest link in the system. Our objective is to develop a robust diagnostic system that has the capability of accurately detecting the state of the drive and correctly locating faults as soon as they occur. We present a machine learning approach to train a diagnostic system, fault diagnostic neural network (FDNN), that detects and locates faulty switch or switches in the inverter. When a fault occurs, the FDNN can point out which switch or switches failed, and so the system can be shut down properly or it may lead to the reconfiguration of the system based on the nature of the fault. In other words, the diagnostic results provided by the FDNN can be used to make a gracefully degradable [9], [10] operation of a faulty drive possible.

Fault diagnostics for internal combustion (IC) engine vehicles has been well investigated [11]–[15], but not to the same extent for electric or hybrid vehicles. However, there are active researches in electrical system diagnostics [16]–[25]. Rule-based expert systems and decision trees are two traditional diagnostic techniques, but they have serious limitations. A rule-based system often has difficulties in dealing with novel faults and acquiring complete knowledge to build a reliable rule base, and is system dependent. A decision tree can be very large for a complex system, and it is also system dependent such that even small engineering changes can mean significant updates [18]. More recently, model-based approaches, fuzzy logic, artificial neural networks (ANNs), and case-based reasoning (CBR) are popular techniques used in various fault diagnostic problems in electrical systems. Moseler and Isermann [16] described a model of black box type using a polynomial differential algebraic equation with application to a brushless dc machine. In their work, the estimated system parameters under normal and faulted conditions are compared with the current system parameter values, and if any discrepancy with normal condition is seen, then a faulty condition is declared. However, the parameter-estimated model of this kind can easily lose the intuitive focus of the system, and in general, does not point toward the specific problem and its location. In addition, sometimes the model can encounter a topological change after a fault, and hence, the premises based on which the model was originally

Manuscript received January 18, 2005; revised August 19, 2005. Recommended by Technical Editor M.-C. Tsia. This work was supported in part by the U.S. Army RDECOM-TARDEC ILIR (In-house Laboratory Independent Research) program.

Y. Murphey, Z. Chen, and B. Zhang are with the University of Michigan-Dearborn, Dearborn, MI 48128-1491 USA (e-mail: yilu@umich.edu).

M. Abul Masrur is with the U.S. Army Tank-Automotive Research Development and Engineering Center, Warren, MI 48397-5000 USA (e-mail: masrura@tacom.army.mil).

Digital Object Identifier 10.1109/TMECH.2006.875568

developed and the parameters estimated may not hold anymore. Ribeiro *et al.* [17] investigated four different techniques for fault detection in voltage-fed asynchronous machine drive systems, all based on direct comparisons of the measured voltages to their reference voltages obtained from the PWM reference signals. Fenton *et al.* [18] gave an overview on the fault diagnostics of electronic systems and emphasized on the need for automated diagnostic tools such as ANN, fuzzy logic, etc. In particular, they recommended hybrid solutions such as model-based approaches combined with CBR, or fuzzy logic or ANN. Kim and Parlos presented a model-based fault detection and diagnosis system for electric motors [19]. Their system used a transient empirical predictor modeled by dynamic recurrent neural networks and wavelet packet decomposition. Their diagnosis system was tested on a 373-kW and a 597-kW induction motor, and its diagnostics accuracy reached about 93%. Filippetti *et al.* [20] investigated the applications of various artificial intelligence (AI) techniques to induction motor drive fault diagnostics. They presented an ANN architecture to quantify a stator short-circuit condition and a fuzzy logic system for the detection of broken rotor bars' fault severity, with an adaptive fuzzy neural network applied to stator short-circuit detection. Zidani *et al.* [21] presented a fuzzy logic system for induction motor stator fault diagnosis based on the stator current Concordia patterns. One fuzzy output is used to assess the fault severity in four conditions in fuzzy terms: zero, light, medium, and high. A comprehensive list of books, workshops, conferences, and journal papers related to induction motor fault detection and diagnosis can be found in [22] and a good discussion on ANN and fuzzy logic methodologies for studying faults in the motor and mechanical faults can be found in [23].

Two quite different approaches used in fault diagnostics in electric motors and drives have also influenced our research. In [24], Kastha and Bose systematically described the effect of different types of fault in a voltage-fed PWM inverter induction motor drive that uses the open-loop volts/hertz speed control method. The important fault types, including single line to ground, rectifier diode short circuit, and earth fault on dc bus, were identified in the beginning and followed by preliminary analysis of the selected fault types. A systematic simulation study was then conducted to substantiate the analytical study. Kastha and Bose pointed out that the study of fault performance of the drive system is extremely complex. The complexity is further aggravated due to a modeling problem of the machine under saturation and unsymmetrical condition. Smith *et al.* presented a time-domain response-based method for the online detection of the intermittent misfiring of the switching devices in a voltage-fed PWM inverter [25]. They pointed out that the frequency domain methodologies are not suitable for the purpose and that time-domain techniques are considered more appropriate.

Our research is one step ahead of those published works. Whereas most of the existing diagnostic systems are built to detect a faulty condition against the normal condition, very few addressed small classes of faulty conditions. We are investigating an advanced machine learning technology combined with a model-based approach for the development of a robust diagnostic system that has the capability of detecting and locating multiple classes of faults in an electric drive operating at any valid (torque, speed) conditions.

Faults in electric drives can be classified into two basic groups: 1) motor related and 2) power electronics related. Among the motor-related faults are included mechanical and electrical faults. Mechanical faults are related to motor bearings and other mechanical unbalances leading to vibrations. Electrical faults within the motor such as partial/full winding (including inter-turn) short circuit, open circuit, etc., and an unbalanced inverter output applied to the motor can all result in unbalanced current and magnetic field in the motor. Power electronics faults are related to inverter failure, e.g., open- or short-circuited switches, or reverse diodes. Such faults can be of either permanent nature or intermittent type. As mentioned earlier, this research is focused on the problem of power electronics inverter fault diagnostics. A power electronics inverter can have a single-switch failure (open or short), a reverse diode failure (open or short), or a multiple of these faults. However, the probability of multiple failures is much lower than single failure event. Other inverter failures can be caused by break down of leads, shorting, or connector problems. In this paper, we focus on the classification of inverter open-circuit faults in switches using a machine learning technology. The techniques presented in the paper are general and can be easily extended to detect other types of faults, either electrical and/or mechanical. We want to point out that in the cases of simple discrete open faults (or short-circuit faults), the signatures can be significantly different from normal conditions and such faults can sometimes be detected by simple methods such as rule-based algorithms. However, our methodology is general enough to detect different classes of faults occurring at different locations, which can be intermittent, and whose signatures may be subtle involving a multiple signal analysis. As we will see later in this paper, such faults are difficult to detect and locate with 100% accuracy. Furthermore, our approach shows that a fault diagnostic system can be developed using machine learning techniques on simulated data, and it performs fault diagnostics robustly under any valid operation conditions.

With the above perspective, the research presented in this paper has the following distinct features compared to the existing techniques.

1) It combines a model-based diagnostics approach with a machine learning technique to train a robust fault diagnostic system.
2) The resulting fault diagnostic system has the capabilities of detecting and locating up to ten different classes of faults in a six-switch inverter. Signal signatures of a faulty condition against the normal condition are relatively easy to identify, whereas the signal signatures of one fault against another fault are often subtle, and not easy to detect.
3) During the development phase of a fault diagnostic system, there is no need to take direct measurements of data from electric drives, which is time consuming and costly.
4) The resulting system has been validated using the data generated by an experimental inverter-motor system and proven to be effective.

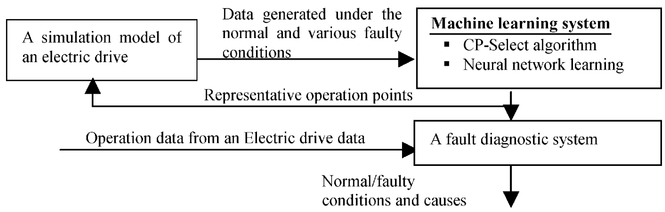

Fig. 1. Model-based fault diagnostic system driven by machine learning.

Fig. 1 illustrates our approach to fault diagnostics of electric drive. "SIM_drive," a simulation model of a field-oriented control (which can be closed or open loop) electric drive with a power-electronics-based inverter and a three-phase induction motor is developed and implemented using the Matlab–Simulink software. SIM_drive has the capability of simulating the normal operation condition of an electric drive as well as the faulty conditions of the open- and post-short-circuit faults in an inverter switch. A post-short-circuit fault implies that if a particular switch of the inverter is short circuited, very shortly thereafter the other inverter switch located on the same limb will be gated to turn on, leading to a complete short circuit of the limb. Eventually, the complete limb where the short circuit occurred will burn out to become permanently open. In our on-going work, we extended the problem scope to include a short-circuit fault where it is assumed that the inverter will be shutdown by a proper protective mechanism when the current exceeds a certain threshold. We have found that our methodology works successfully on these faults as well, and we plan to report this in a subsequent paper.

In the SIM_drive model, we assume a minimal amount of current and voltage sensors available in a drive system: current sensors in series with any two of the inverter output lines and two voltage sensors across any two of the output terminals of the inverter. The SIM_drive model operates at any selected (torque, speed) operating point under normal and various faulty conditions. Since in real world, an electric drive can operate at different (torque, speed) points, a diagnostic system should be trained to be robust throughout the (torque, speed) domain. A machine learning algorithm is developed to select representative operating points from the (torque, speed) domain for use by the SIM_drive model to generate training data. The objective of the machine learning approach is to train a diagnostic system on the representative data so that it has the capability of performing accurate fault diagnostics in an electric drive that operates at any valid operating point. The intelligent system used in this research is a multiclass neural network system. We will describe two possible neural network architectures and discuss their pros and cons. It should be noted that once a model-based ANN has been trained, its implementation in a real-time environment is rather simple, since it amounts to having just the weights of the neurons in the ANN burnt in an inexpensive microprocessor.

Experiments were conducted on both the simulated data and the data generated by an experimental bench setup. The results show that the proposed diagnostic system is very effective in detecting multiple classes of faulty conditions of an inverter in an electric drive operating at any valid (torque, speed) point.

II. Three-Phase Electric Drive Model

In this section, we briefly describe the basics in the development of a simulation model of an electric drive. The structure of the electric drive system using an induction motor with an optional closed loop is shown in Fig. 2(a). The inputs to the system are the dc voltage, reference torque, reference air gap magnetic flux in the induction motor, and the mechanical source/sink input in the form of shaft speed or load torque in the shaft. The controller is an FOC [3]–[7] that generates a reference three-phase voltage. This reference voltage is then synthesized through a PWM process. In the open-loop configuration, the feedback torque loop shown in Fig. 2(a) does not exist, and the controller simply generates a voltage and a frequency reference using any scheme, which can include, among others, constant volts per hertz (V/Hz). The motor is represented by the following standard set of equations with d–q axis fixed in the stator [3], [5]–[7]:

$$V_{ds} = (R_{\mathrm{s}} + pL_{\mathrm{s}})I_{d\mathrm{s}} + \mathrm{p}\mathrm{M}I_{d\mathrm{r}} \tag{1}$$

$$V_{qs} = (R_{\mathrm{s}} + pL_{\mathrm{s}})I_{q\mathrm{s}} + pMI_{q\mathrm{r}} \tag{2}$$

$$0 = pMI_{d\mathrm{s}} + \omega_{\mathrm{r}}MI_{q\mathrm{s}} + (R_{\mathrm{r}} + pL_{\mathrm{r}})I_{d\mathrm{r}} + \omega_{\mathrm{r}}L_{\mathrm{r}}I_{q\mathrm{r}} \tag{3}$$

$$0 = -\omega_{\mathrm{r}}MI_{d\mathrm{s}} + pMI_{q\mathrm{s}} - \omega_{\mathrm{r}}L_{\mathrm{r}}I_{d\mathrm{r}} + (R_{\mathrm{r}} + pL_{\mathrm{r}})I_{q\mathrm{r}} \tag{4}$$

where R_{s} and R_{r} are stator and rotor resistances, L_{s} and L_{r} are stator and rotor self-inductance, M is the stator/rotor mutual inductance, ω_{r} is the electrical rotor angular velocity, $V_{d\mathrm{s}}$ and $V_{q\mathrm{s}}$ are d- and q-axis stator voltages, $I_{d\mathrm{s}}$ and $I_{q\mathrm{s}}$ are d- and q-axis stator currents, $I_{d\mathrm{r}}$ and $I_{q\mathrm{r}}$ are d- and q-axis rotor currents, and p is the differential operator d/dt. The rotor is assumed to be shorted and hence the voltages are 0 in (3) and (4). The electromagnetic torque is defined as $T_{\mathrm{e}} = (3/2)(P/2)M(I_{q\mathrm{s}}I_{d\mathrm{r}} - I_{d\mathrm{s}}I_{q\mathrm{r}})$, where P is the number of poles. In an FOC scheme, this torque equation can be simplified further by dropping the second term within the parenthesis leading to a simple control [3]. The mechanical equation of motion for the motor shaft is given by $T_{\mathrm{e}} - T_{\mathrm{L}} = P/2[J(d\omega_{\mathrm{m}}/dt) + B\omega_{\mathrm{m}}]$, where ω_{m} is the mechanical shaft speed, the excitation frequency $\omega = (P/2)\omega_{\mathrm{m}}, T_{\mathrm{L}}$ is the load torque, J is the moment of inertia, and B is the friction coefficient. These equations are numerically solved for currents during the implementation of a simulation model using Matlab–Simulink. Specifically, we intend to simulate various faults for the six-switch scheme shown in Fig. 2(b).

One possible approach for fault diagnosis in an inverter is to have sensors installed at all possible locations to flag any abnormalities, assuming that the sensors do not fail as well. For example, to detect open-circuit fault conditions within an inverter, we would need to place current sensors at every single switch and a reverse diode to detect whether a particular switch or diode is faulty. This is not cost-/weight-effective, and real-life inverters do not contain that many sensors. Our approach assumes that only a minimal amount of current and voltage sensors exist in an electric drive system: The current sensors in series with any two of the inverter output lines, and two voltage sensors across any two of the output terminals of the inverter. We also assume a Y-connected three-phase induction motor stator, without any return connection from the neutral point of Y.

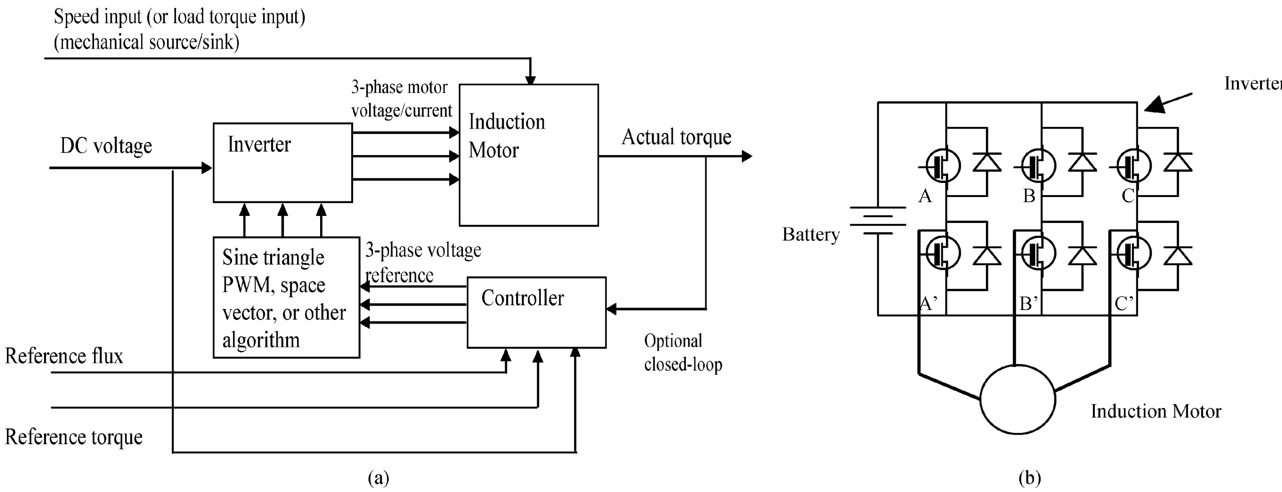

Fig. 2. (a) Three-phase electric drive model and (b) six-switch inverter in a three-phase electric drive.

TABLE I
SWITCHING TABLE FOR NORMAL OPERATION OF THE SWITCHES

STATE #	SWITCH A	SWITCH B	SWITCH C	Van / V	Vbn / V	Vcn / V
Null	0	0	0	0	0	0
1	0	1	0	-1/3	2/3	-1/3
2	0	1	1	-2/3	1/3	1/3
3	0	0	1	-1/3	-1/3	2/3
4	1	0	1	1/3	-2/3	1/3
5	1	0	0	2/3	-1/3	-1/3
6	1	1	0	1/3	1/3	-2/3
Null	1	1	1	0	0	0

TABLE II
SWITCHING TABLE FOR THE FAULTED OPERATION IN WHICH SWITCH A IS PERMANENTLY OPEN

STATE #	SWITCH A	SWITCH B	SWITCH C	Van / V	Vbn / V	Vcn / V
Null	0	0	0	0	0	0
1	0	1	0	-1/3	2/3	-1/3
2	0	1	1	-2/3	1/3	1/3
3	0	0	1	-1/3	-1/3	2/3
4	0	0	1	-1/3	-1/3	2/3
5	0	0	0	0	0	0
6	0	1	0	-1/3	2/3	-1/3
Null	0	1	1	-2/3	1/3	1/3

The problem statement can thus be summarized as follows: *For a six-switch inverter driven three-phase induction motor embedded with two current sensors in the output inverter lines and two voltage sensors across the lines, a robust diagnostic system is to be developed to accurately identify any single faulty inverter switch among the six switches, or one failed vertical switch pair*.

The above-mentioned theoretical model was implemented in a simulation model, SIM_drive, using the Matlab–Simulink software. SIM_drive has the capability of simulating the normal and faulty operations within the three-phase induction motor drive at any given (torque, speed) point. Table I shows the normal operation of the scheme shown in Fig. 2(b). The numbers in the voltage columns are to be multiplied with the dc voltage V, to obtain the true voltage applied to the motor phase windings. In the implementation, we assume that a gating signal 1 implies that the switch is turned on and 0 implies that the switch is turned off. We also assume that if the upper switch A is on, then the lower switch A$'$ will be off, and vice versa, to prevent any possibility of direct short circuit of the dc voltage source. Table II shows the states of the six-switch inverter when the switch A is open faulted. In this case, although switch A (upper limb) is supposedly turned on, in reality, it remains off due to an open-circuit fault. In addition to the six states shown in Table I, we also have two null states corresponding to all switches being on or off simultaneously. These null states amount to short circuiting of the motor terminals. The model is also used to simulate three post-short-circuit cases corresponding to the three vertical switch pairs open, one pair at a time, namely, the pairs A and A$'$, B and B$'$, and C and C$'$, respectively. The operating conditions used in the simulation are specified in Table III.

Fig. 3 shows examples of the simulated signals generated under the normal operation condition by SIM_drive. In Fig. 3(a), the step function is the command torque and the actual torque is seen to ultimately follow the command with a delay depending on the controller settings. Fig. 3(b) shows the current signals $I_{\rm a}$, $I_{\rm b}$, and $I_{\rm c}$. Fig. 4 shows the signal behaviors with switch A open circuited at time 0.1 s. Fig. 4(a) shows the torque command (step function) and the actual torque signal (oscillatory with changing amplitude). Fig. 4(b) shows the currents $I_{\rm a}$, $I_{\rm b}$, and $I_{\rm c}$ (three currents in different shadings, with 120° phase shift from each other in a steady state) acquired after the fault. Note that we used a short trigger time for the purpose of clarity in viewing the faulty signal features. It should also be noted that in simulations, no restriction was imposed on the current magnitude, whereas in an experimental system, there is a limit to the allowable current to prevent any damage to the system or the components.

TABLE III
OPERATING CONDITIONS USED IN THE SIMULATED SINE-PWM-CLOSED-LOOP MODEL.

Variable name	Description	Value
V_{DC}	DC voltage provided by battery	500V
PWM carrier frequency	Frequency of the sine wave	8 kHz
Speed	Fixed running speed of the motor	60, 300, 600, 900, 1800 rpm
Reference torque command	Mechanical torque desired from the motor	10, 50, 100, 200 Nm
Simulation time	Simulation time	6.25s
Trigger time	Time point to trigger the fault condition	0.25s
Sampling rate	Sampling rate to get the output data.	0.001s
Points of data	Points of data	6000

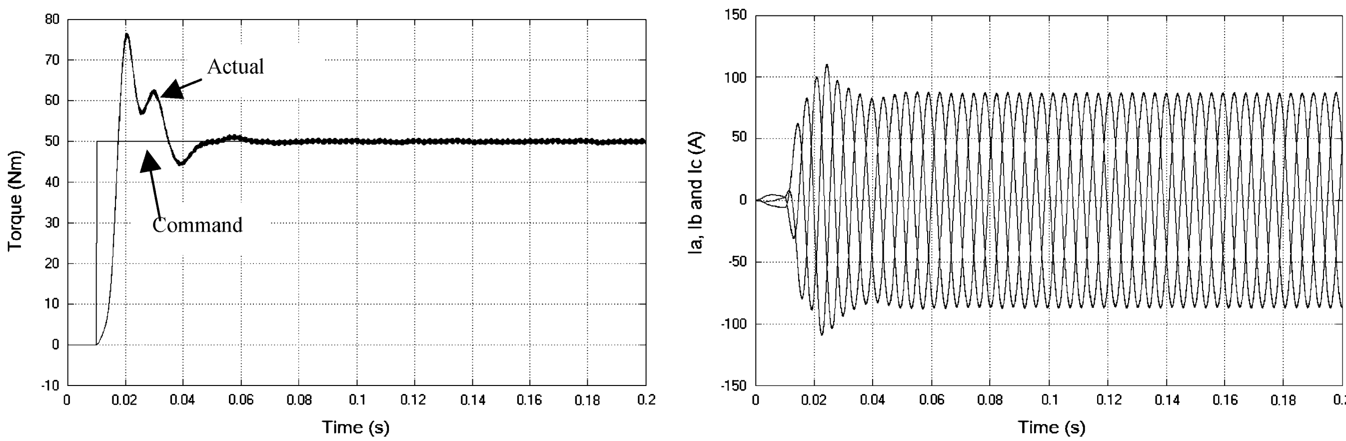

(a) (b)

Fig. 3. Signal behaviors in the normal condition generated by SIM_drive. (a) Torque signal. (b) $I_{\rm a}$, $I_{\rm b}$, and $I_{\rm c}$ signals.

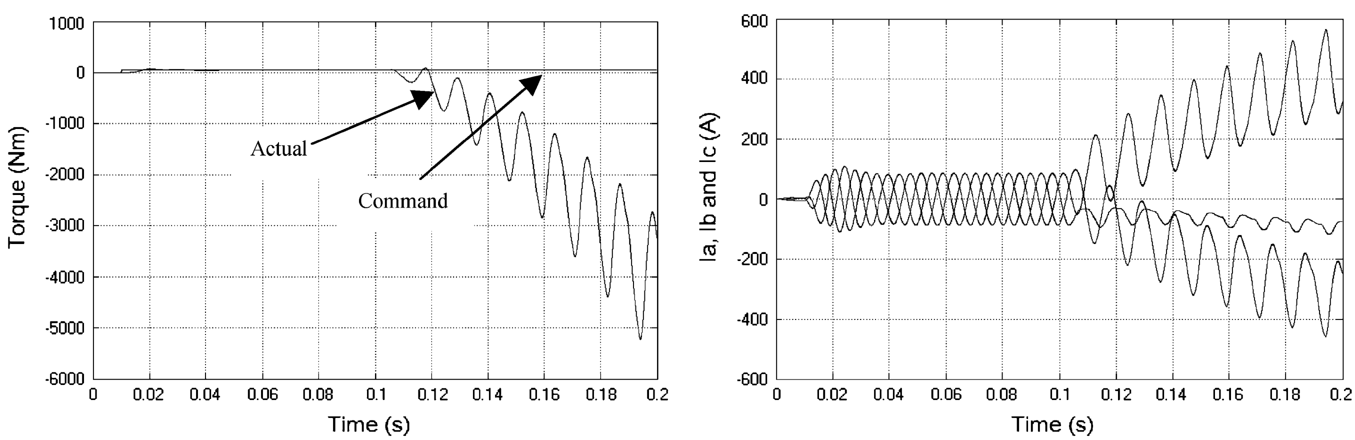

(a) (b)

Fig. 4. Signal behaviors generated by SIM_drive in a condition that switch A is open. (a) Torque signal. (b) $I_{\rm a}$, $I_{\rm b}$, and $I_{\rm c}$ signals.

Fig. 5 shows the signal behaviors of one post-short-circuit case in which the pair A and A′ becomes open circuited at time 0.25 s. As discussed earlier, short-circuiting switch A made A′ open eventually, since the latter is gated to be on, shortly after the short circuit, causing the entire A and A′ limb to become open.

III. ELECTRIC DRIVE FAULT DETECTION USING SIGNAL ANALYSIS AND MACHINE LEARNING

Fault diagnostics in an electric drive can be performed by developing an intelligent system that can learn to detect signal faults under various faulty circuit conditions. The challenges in developing such robust diagnostic systems lie in the fact that it is easier to identify signatures of a faulty condition against the normal condition, whereas signal signatures of one fault against the another one are often quite subtle. We model the fault diagnostics in the electric drive as a multiclass classification problem. The input space consists of relevant signals (e.g., voltages and currents among others) from the electric drive system, and the output space consists of the class labels $\{f_0, f_1, \ldots, f_k\}$, where f_0 is considered to be the normal operational condition and f_1 through f_k are the k faulty conditions in the electric drive, which in our case correspond to the six switches, one open at a time, and the three cases of post-short circuits. Fig. 6 illustrates the computational steps involved in

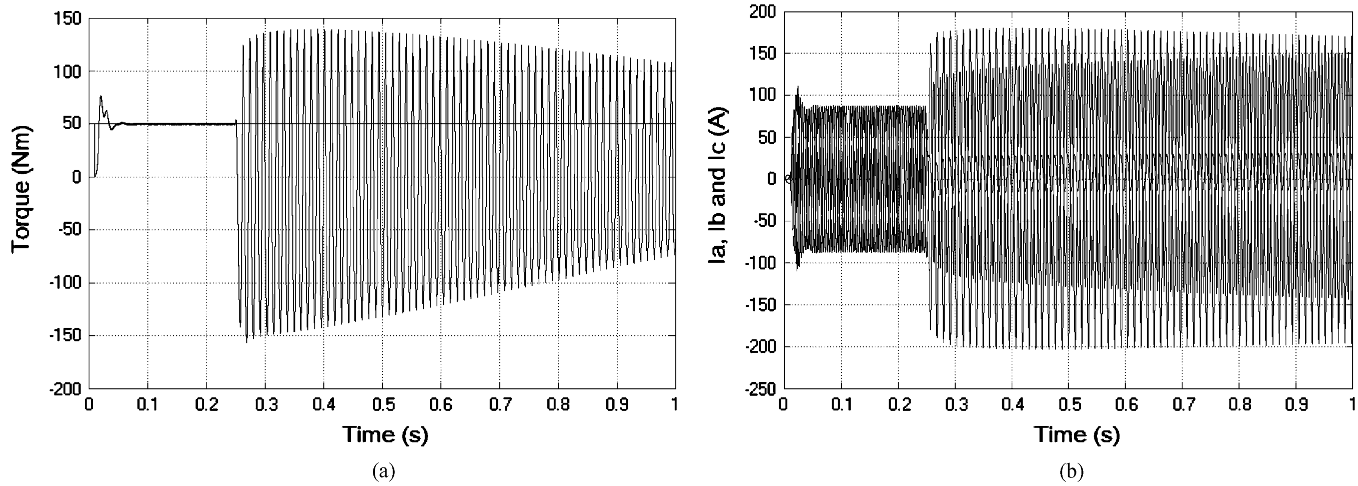

Fig. 5. Signal behaviors in an abnormal condition that both switches A and A′ are open in a sine-PWM-closed-loop model. (a) Torque signal. (b) I_a, I_b, and I_c signals.

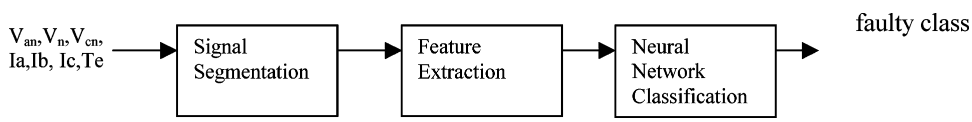

Fig. 6. Major computational steps in a signal fault detection system.

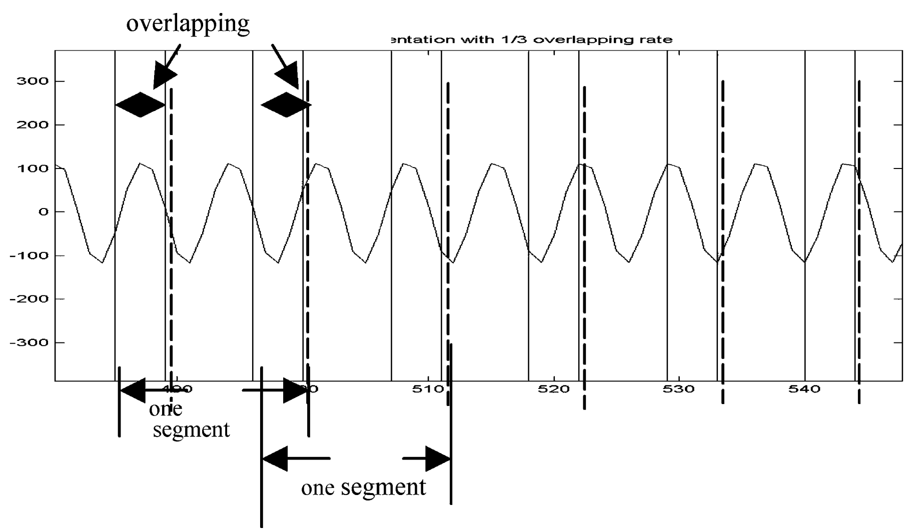

Fig. 7. Signal segmentation.

the signal fault detection system, where the input consists of the voltages V_{an}, V_{bn}, V_{cn} to the motor, the currents I_a, I_b, and I_c, and the motor electro-magnetic torque T_e. Note that we use time-domain signals instead of frequency-domain signals in our diagnostic system for the same reasons as indicated by Smith *et al.* [25]. The first computational step is to segment the signals and extract the signal features from each segment. The signal segments are then analyzed by an ANN, which is trained on the signals generated by SIM_drive at the parameter points selected by the Control Point-Select (CP-Select) algorithm, a machine learning algorithm. The major research contribution in this section is the machine learning technology used to train a neural network that can robustly detect and locate faults inside an electric drive operated under any given valid condition.

A. Signal Segmentation and Feature Extraction

Signal fault detection is performed on a segment-by-segment basis. All input signals are segmented using the same fixed sized segments and the two adjacent segments are overlapped in one-third of the segment width to maintain continuity of information flowing between segments. The basic frequency of the signals is over 80 Hz, and sampling frequency is chosen to be 1000 Hz, which is sufficient for this purpose. We chose to use 16 samples in each segment with an overlap of 5 samples between 2 adjacent segments. A signal of 3000 data samples is segmented into 272 segments. Fig. 7 illustrates the segmentation scheme. The solid vertical lines indicate the beginning of segments, the dashed vertical lines indicate the ending of segments, and the signal between a dashed line and the subsequent solid line is

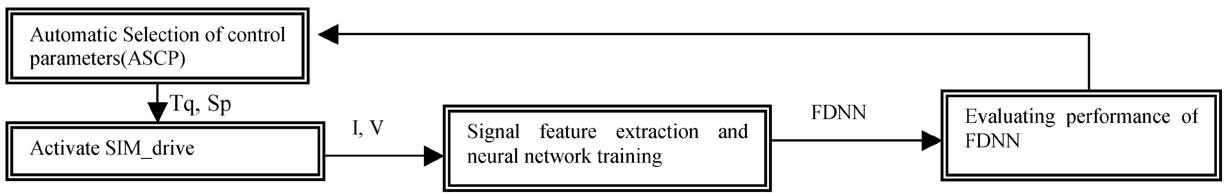

Fig. 8. CP-Select algorithm for an electric drive diagnostic system.

the overlapping portion of the two adjacent segments. Each signal segment is represented by the following features.

- Max: maximum magnitude of the signal within the segment.
- Min: minimum magnitude of the signal within the segment.
- Median: median of the signal within the segment.
- Mean: mean of the signal within the segment.
- Standard deviation: standard deviation of the signal segment.
- Zero-frequency component of the power spectrum.

The detection of signal faults within a time period requires one segment from each input signal and each segment is represented by the six features listed above. Since we have seven input signals (three voltage signals, three current signals, and one torque signal), the combined feature vector to represent a particular state in the electric drive at a particular time is a vector of 42 dimensions. The feature vector is the input to a neural network classifier that determines whether the seven signals within this time period manifest any fault.

B. Smart Selections of Operation Parameters

In a drive system, the current and voltage signals behave differently under different operating conditions specified by torque and speed. The issue of smart selection of "control parameters" (also referred to as operating point) in the (torque, speed) domain is important for all electric drive diagnostic systems that are trained on simulated data.

A diagnostic system trained on more representative data is more likely to perform better diagnostics in real world system under any operation condition. Fig. 8 illustrates the proposed machine learning algorithm, CP-Select, for the generation of a robust electric drive diagnostic system. The CP-Select algorithm automatically selects representative operating points in a given domain of control parameter space to generate representative training data for a neural network system for fault diagnostics. The operating space for a drive system has two components, i.e., torque (Tq) and speed (Sp). The Tq and Sp pair selected by CP-Select is sent to SIM_drive, which in turn, generates current and voltage signals I and V, at all three phases at the given speed and torque point under the normal and faulty conditions. Collectively, these signals are denoted as $\mathbf{I}, \mathbf{V}$, where $I = \{I_0, I_1, I_2, \ldots, I_k\}$ and $V = \{V_0, V_1, V_2, \ldots, V_k\}$, where the elements I_i and V_i (with $i = 0$ to k) within the $\mathbf{I}$ and $\mathbf{V}$ vectors are current and voltage signals obtained under normal (with index 0) and k faulty conditions. I_i and V_i themselves can be vectors that contain several signals acquired at different locations of the circuit. Diagnostic features are extracted from these signals and feature vectors are used to train an ANN called FDNN, and the performance of the FDNN is evaluated on a validation data set Tv. If the performance is satisfactory, the algorithm stops; otherwise, more operating points are selected. Tv is a validation data set containing features extracted from signals generated by SIM_drive that operates on a set of randomly selected control parameters (operating points) in the (torque, speed) domain.

The most complicated component in the CP-Select algorithm is automatic selection of control parameters (ASCP). Initially, Φ contains the rectangular space (refer to Figs. 9 and 10) that includes all valid torque and speed points used by a real world electric drive. As the process goes on, Φ contains all subspaces from which potential parameters can be selected. The ASCP algorithm repeatedly removes one parameter space from Φ at a time and performs an iterative process until Φ is empty or the performance of the trained FDNN is satisfactory. At each iteration ASCP selects three sets of points, and each set goes through a simulation, training, and evaluation process as shown in Fig. 9. The first set of points contains the four corner points and the center point of the current parameter space C_CP (see X_1, X_2, X_3, X_4, and X_5 in Fig. 10) and are stored in P_0. The points in P_0 that have not been selected before are sent to SIM_drive to generate new training data. The newly generated training data are combined with the existing ones to form the current training data set Tr. The FDNN is trained on Tr and evaluated on validation data set Tv. If the performance of the FDNN on Tv is satisfactory, the process stops. Otherwise it goes on to select the second set of points, which are the interior points of the current parameter space C_CP (see X_6, X_7, X_8, and X_9 in Fig. 10). The same simulation, training, and evaluation steps are repeated on this set of points. If the performance of the FDNN at this stage is satisfactory, the process stops. Otherwise, the third set of parameters is selected, which contains the four center points on the four sides of C_CP (see X_{10}, X_{11}, X_{12}, and X_{13} in Fig. 10). Again, the same simulation, training, and evaluation process is applied to this set of parameters as well. If the performance of the FDNN at this stage is satisfactory, the ASCP algorithm stops; otherwise, the current parameter space C_CP is evenly divided into the four subspaces $\mathrm{CP}_1, \mathrm{CP}_2, \mathrm{CP}_3$, and CP_4, which are appended to the parameter space set Φ. All the parameter spaces in Φ are sorted based on the performances of the FDNN on the validation points in the space, and then the entire process is repeated.

We have conducted an experiment to evaluate the CP-Select algorithm by using the SIM_drive described in Section II. We identified a valid (torque, speed) space as {Torque (Nm): [10, 200], Speed (rpm): [50, 1800]} an initial space denoted as C_CP.

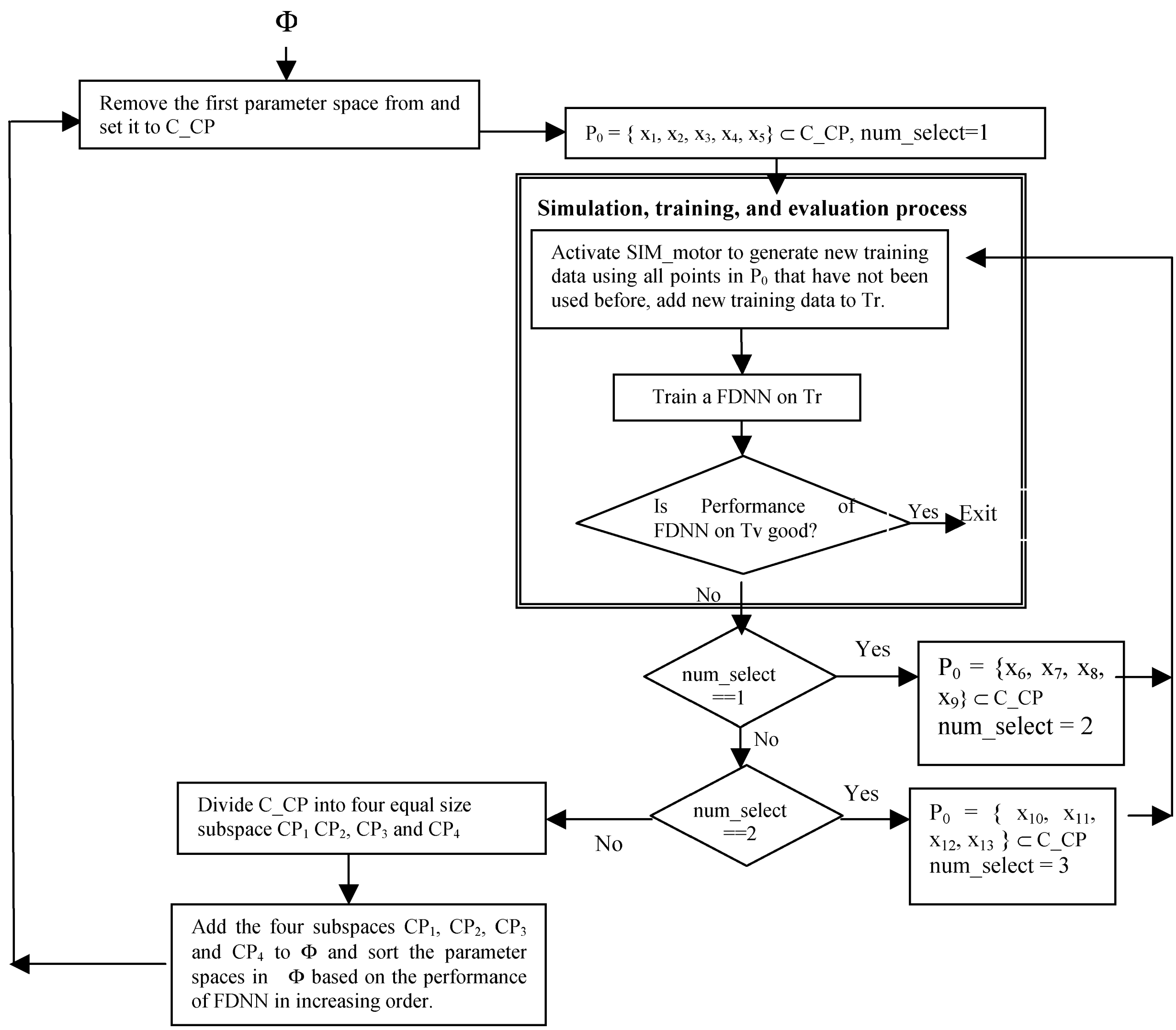

Fig. 9. Computational steps in ASCP component (refer points $x_i, i = 1, \ldots, 13$, in Fig. 10).

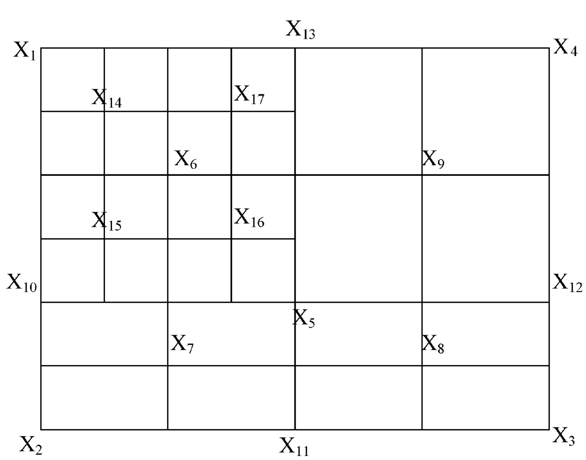

Fig. 10. Operating points in a two-dimensional CP space.

For every pair of (torque, speed) points (Tq, Sp) selected by the CP-Select algorithm, we ran the simulation model for about 6 s to generate seven sets of current and voltage signals in the three phases. One set is normal signal series, and each of the other six sets corresponds to one faulty condition. All these signals are segmented and signal features are extracted, and an FDNN is trained to classify the single-switch faults in the inverter in an electric drive. The CP_Select algorithm selected eight random points within the C_CP space to form the (torque, speed) validation set $\text{Tv} = \{(25, 236), (75, 360), (36, 1149), (96, 1502), (121, 119), (135, 518), (146, 672), (176, 1401)\}$, which are shown by cross marks in Fig. 11. The points shown by diamonds were selected at the first iteration, and the points marked by squares and triangles were generated by the CP-Select algorithm at the second and third iterations, respectively. The points marked by asterisks are the randomly selected test data. Fig. 12 shows the performance of a six-class neural network system trained to classify the single-switch faults in a three-phase inverter. The performance was obtained by evaluating the neural network on the validation set Tv after it is trained on at each iteration. We chose to use performance threshold per_th $= 99\%$. At the first iteration, training data Tr_0 contains signal data generated by SIM_drive on the control points selected in the first iteration (see Fig. 11). A neural network FDNN0 is trained on Tr_0 and the overall performance of FDNN0

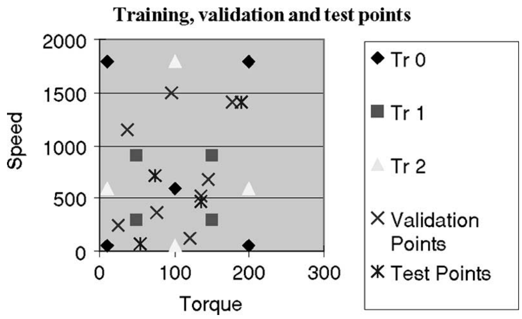

Fig. 11. Randomly selected test and validation set, and the train data selected by CP-Select algorithm.

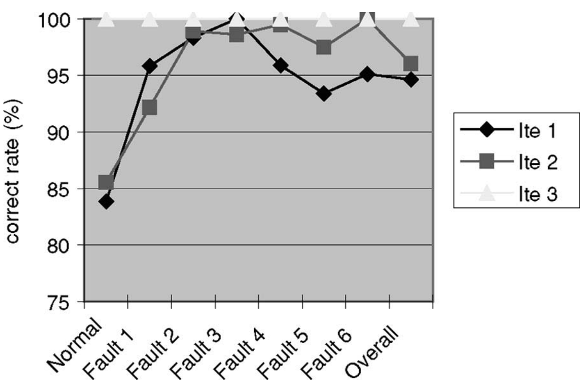

Fig. 12. Performance of the FDNN trained on data generated by SIM_drive using the control points generated by the CP-Select during three iterations. (a) A system of two neural networks for classifying the single-switch and short-circuit faults in a three-phase electric drive. (b) A ten-class single neural network for classifying all ten classes of faults in a three-phase electric drive.

evaluated on the validation set is $94.62\% < \text{Perf\_th} = 99\%$. Its performance on individual classes is shown in the curve connecting the diamond-shaped points in Fig. 12. At the second iteration, the FDNN is trained on $\text{Tr}_0 \cup \text{Tr}_1$, where Tr_1 is the signal data generated by SIM_drive on the points selected by the CP_Select at the second iteration, and its performance on Tv is shown in the curve connecting the square points in Fig. 12. The overall performance is $96.06\% < \text{Perf\_th} = 99\%$. At the third iteration, the FDNN is trained on $\text{Tr}_0 \cup \text{Tr}_1 \cup \text{Tr}_2$, where Tr_2 is the signal data generated by the SIM_drive on the points selected by the CP_Select at the third iteration, and its performance on Tv is shown in the curve connecting the triangular points in Fig. 12. The overall performance at the third iteration is $100\% > \text{Perf\_th} = 99\%$; therefore, the algorithm stops.

C. Multiclass Fault Classification Using ANNs

ANNs are capable of capturing underlying numerical or logical relationships among training examples. Neural networks have successfully been applied to a broad range of problems, including engineering diagnosis, pattern classification, intelligent manufacturing, control problems, and computer vision [25]–[34]. A neural network architecture using feedforward backpropagation consists of specification of the number of layers, number of units in each layer, type of activation function of each unit, and the connection weights between the units of different layers, which are determined by a machine learning algorithm. According to Huang *et al.* [30], two-layer or sometimes called one-hidden-layer perceptrons can implement any convex open or closed decision regions. Therefore, we chose to use a one-hidden-layer architecture for signal fault detection. Most of the research in neural networks has been in the development of learning and training algorithms for two-class classifiers, i.e., classifiers with one output node that represent classes 0 and 1. However, fault diagnostics in electric drive has six classes of single-switch faults and three classes of post-short-circuit classes. The most common architectures, which have been proposed for multiclass neural networks [35], involve a single neural network with K output nodes, where K is the number of faulty classes, and a system of binary neural networks combined with a posterior decision rule to integrate the results of neural networks. A system of binary neural networks requires separate training of each neural network, and each trained neural network generates a decision boundary between one class and all others. The most notable limitation in this approach is that the decision boundaries generated by the different two-class neural network classifiers can have overlapped or uncovered regions in the feature space [35]. For the feature vectors that fall on an overlapped region in the feature space, more than one two-class classifiers can claim the input as its classes, resulting in ambiguity. The feature vectors falling on the regions that are not claimed by any neural networks will be rejected by all neural networks. As a result, the resulting system may not generalize well. Another type of multiclass neural network system uses a single neural network with k output, where $k > 1$. This type of the neural network architecture has the advantage of simple training procedure, and only one neural network is trained for all m classes, where $m > 2$. If trained properly, a neural network system implemented in this architecture should reduce the ambiguity problem [35].

Based on the single neural network architecture, we implemented two different systems of neural networks as illustrated in Fig. 13 for the diagnosis of ten classes of faults in an electric drive: one class represents the normal condition, six classes represent six single switch faults, and the last three classes represent the three post-short-circuit faults.

Fig. 13(a) shows a structured diagnostic system consisting of two neural networks, one trained to classify single-switch faults, and the other classifies the post-short-circuit faults, and a winner take all (WTA) [35] approach is used to integrate the results from the two neural networks. Fig. 13(b) shows a single neural network trained to classify all ten classes: Normal, six single-switch faults, and three post-short-circuit faults. One important issue in a multiclass neural network is how to encode the classes in the output nodes of the neural network. In both neural network architectures, we chose to use a "one-hot spot" method described as follows: For a k-class classification problem, we need an output layer of k bits, each class is assigned a unique binary string (codeword) of length k with only one bit set to "1" and all other bits are "0." For example, if it is a six-class classification problem, class 0 is assigned a codeword of 000001, class 1 is assigned a codeword of 000010, class 2 is assigned of a codeword of 000100, etc. The advantage of this encoding is

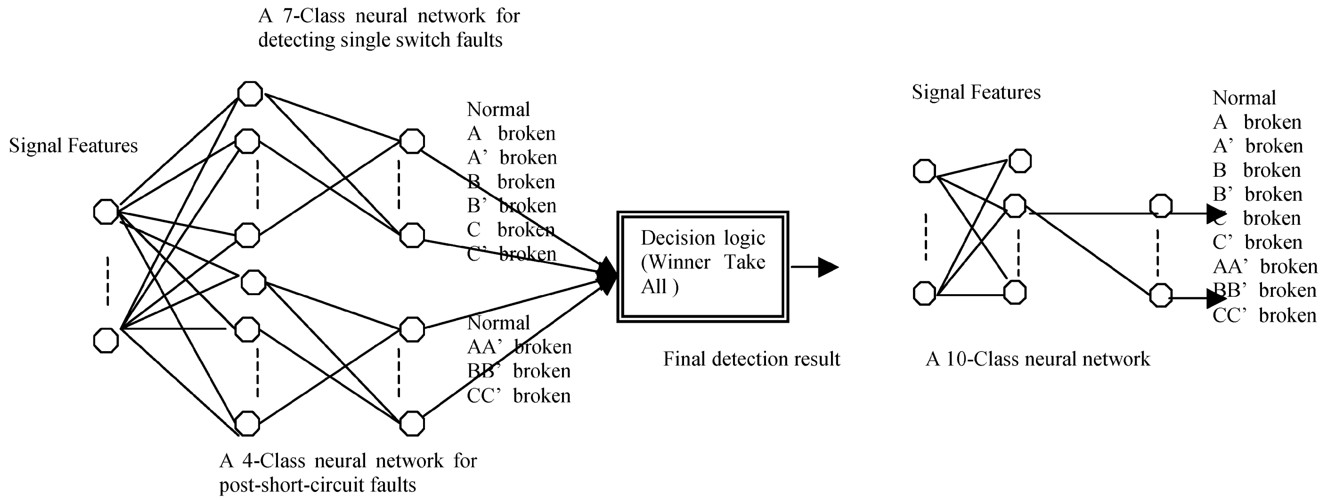

(a) (b)

Fig. 13. Two neural network architectures developed for the fault classification in an electric drive. (a) A system of two neural networks for classifying the single-switch and short-circuit faults in a three-phase electric drive. (b) A ten-class single neural network for classifying all ten classes of faults in a three-phase electric drive.

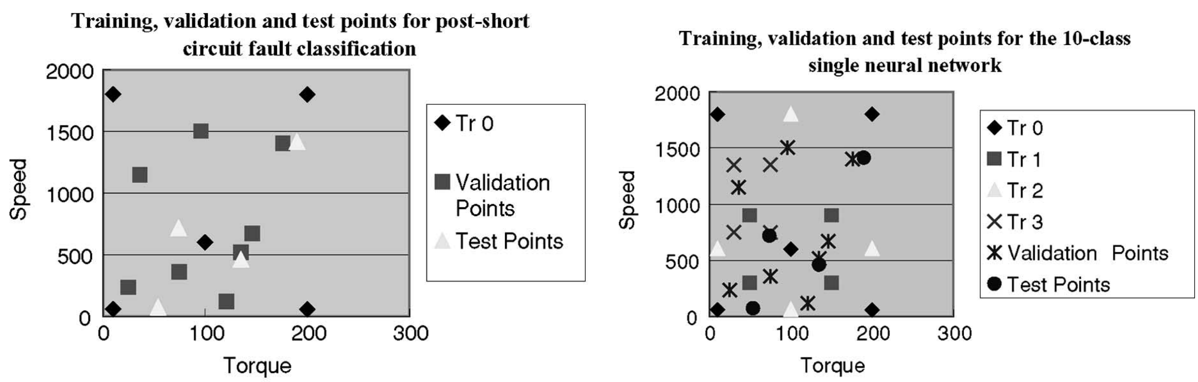

(a) (b)

Fig. 14. (a) Randomly selected test and validation parameters, and the training parameters selected (a) by the CP-Select for classifying post-short-circuit faults and (b) by the CP-Select using a single neural network classification system.

that it gives enough tolerance among different classes. We use the back propagation learning algorithm to train all the neural networks.

To evaluate these two neural network systems, we conducted the following experiments using simulated data. The structured multiclass neural network system contains two separately trained neural networks, both having 42 input nodes and 1 hidden layer with 20 hidden nodes. The neural network for single-switch fault classification has seven output nodes, which represent the normal class and the six faulty classes. The neural network for the post-short-circuit classification has four output nodes, which represent the normal class and the three post-short-circuit classes.

The randomly selected validation and test parameters, and the training parameters generated by the CP-Select algorithm for the six single-switch faults are shown in Fig. 11 and the parameters (operating points) for the post-short-circuit are shown in Fig. 14.

The single-switch fault classification neural network was trained on the control parameters in $\mathrm{Tr}_0, \mathrm{Tr}_1$, and Tr_2 generated by the CP-Select algorithm using three iterations as described in Section III-C. The post-short-circuit fault classification neural network was trained on the control parameters (operating points) in Tr_0 shown in Fig. 14, which gave 100% correct performance on the validation data shown in the squared points in Fig. 14. Therefore, the CP-Select algorithm stopped at the end of the first iteration. The four randomly selected test points are shown by triangle in Fig. 14. For the ten-class single neural network system, the CP-Select algorithm generated the training points in four iterations resulting in $\mathrm{Tr}_0, \mathrm{Tr}_1, \mathrm{Tr}_2$, and Tr_3, which are shown in Fig. 15 along with the validation points and test points. The ten-class neural network has 42 input nodes and 1 hidden layer with 20 hidden nodes, and ten output nodes, where one node represents the normal class, and six nodes represent the single-switch fault classes, and three nodes represent the three post-short-circuit faulty classes. It is trained on the data generated by the SIM_drive using the operating points in $\mathrm{Tr}_0 \cup \mathrm{Tr}_1 \cup \mathrm{Tr}_2 \cup \mathrm{Tr}_3$.

The test data for both diagnostic systems were the signals generated by SIM_drive from the same four (torque, speed) points as shown in Figs. 11 and 14. A total of 11 320 feature vectors

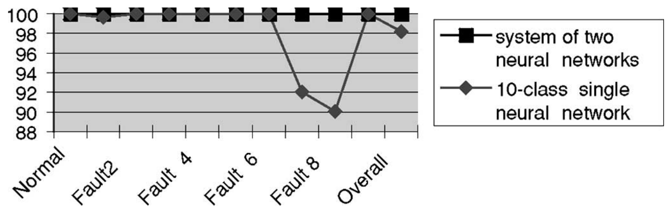

Fig. 15. Performances of two different neural network systems.

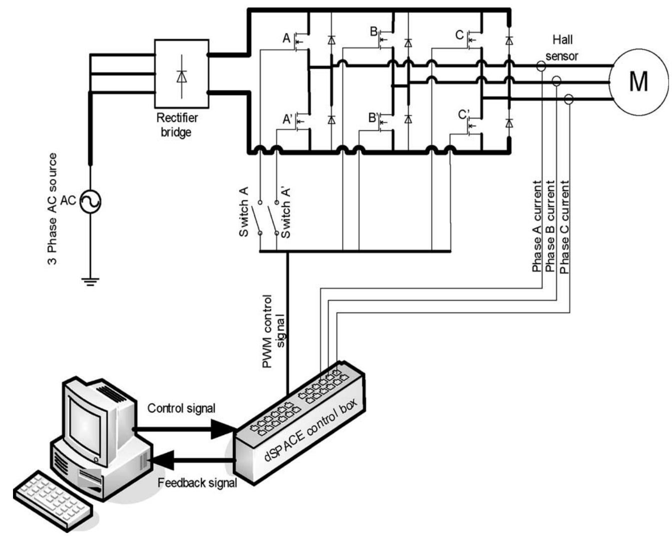

Fig. 16. Experimental setup of the electric drive system.

were extracted from these signals among which 6792 data samples contain the six single-switch faults, and 3396 contain the three post-short-circuit faults, and 1132 are normal. The performances of these two diagnostic systems on the test data set are shown in Fig. 15. The structured diagnostic system correctly detected and located all nine faulty classes and the normal class with 100% correct detection. The single neural network system correctly detected with 100% all the six single-switch faults, but detected correctly with only 90% and 92% on test data from the post-short-circuit faulty class 1 and class 2. We want to point out that if there were signal data on the data generated from real-time operation, the FDNN can be trained by combining the simulated and real-time signals. The resulting FDNN is then expected to be more robust. Since operation data are difficult to obtain at the design stage, it is also possible to train the FDNN using only the simulation data initially, and then incrementally train the FDNN as the real operation data becomes available, which has been discussed in one of our papers [36].

IV. Performance of FDNN on Data Generated from Bench Setup

A reasonable question about model-based diagnostic approaches based on simulation data is how well the system can operate on real data, which often contain noise and are not as stable in the sense that signals generated under the same faulty condition vary in certain features. To evaluate the robustness of the proposed model-based diagnostic system trained through machine learning, we developed an experimental bench setup of an electric drive in the Vehicle Electronics (VE) Laboratory at the University of Michigan-Dearborn (Dearborn, MI) in an attempt to generate data as close to real operation as possible. Fig. 16 shows the system setup and the three-phase open-loop inverter circuit that has the capability of generating signals under the normal and various faulty conditions.

The bench setup has the following components: Matlab–Simulink, dSPACE control desk and control box, Hampden IM-100 induction machine, three-phase transformer, three-phase rectifier, inverter, interface boards, and Hall sensor. The signals generated by the bench setup are not stable in the sense that signals generated under the same faulty condition but at different run can have different behavior. Figs. 17 and 18 show the signals generated in two separate runs by the bench setup system when switch A is broken and both A and A$'$ are broken, respectively. It is obvious that the signals generated by the bench setup under the conditions are not identical in the two separate runs. Fig. 19 shows the $I_{\mathrm{a}}, I_{\mathrm{b}}$, and I_{c} signals generated by a simulated model in which switch A was broken in Fig. 19(a) and both switches A and A$'$ were broken in Fig. 19(b). It is clear that the signals generated by SIM_drive are smooth and have expected behaviors, and the signals generated by the bench setup and SIM_drive are similar but have small variations. A neural network system developed using the machine learning approach described in Section III has been tested on the data generated by the experimental bench setup system shown in Fig. 16 and the results are shown in Fig. 20. The three classes of post-short-circuit fault were detected and located with 100% accuracy. The six classes of single-switch faults were detected and located correctly within 98% of all the cases. The lowest detection rate is on the normal condition, which is close to 96% over all cases.

V. Summary and Conclusions

To effectively detect and locate multiple classes of faults, it is important to develop a diagnostic system that is robust for an electric drive operating at any valid torque and speed. We have presented a model-based diagnostic system framework driven by a machine learning algorithm for multiclass fault detection in an electric drive system with a three-phase induction motor. The framework consists of a simulated model of an electric drive and implemented using Matlab–Simulink, a machine learning algorithm for the smart selection of vehicle-operating points from the (torque, speed) space for use by the simulated model, SIM_drive to generate representative training data, and a neural network classification system developed and trained on the signals generated at the representative operating conditions for the fault diagnostics of electric drive inverters.

The SIM_drive assumes minimum number of sensors and contains control mechanisms for generating current and voltage signals at all switches under the normal operation condition, all single switch broken and post-short-circuit conditions. The simulated electric drive model uses a closed loop field-oriented

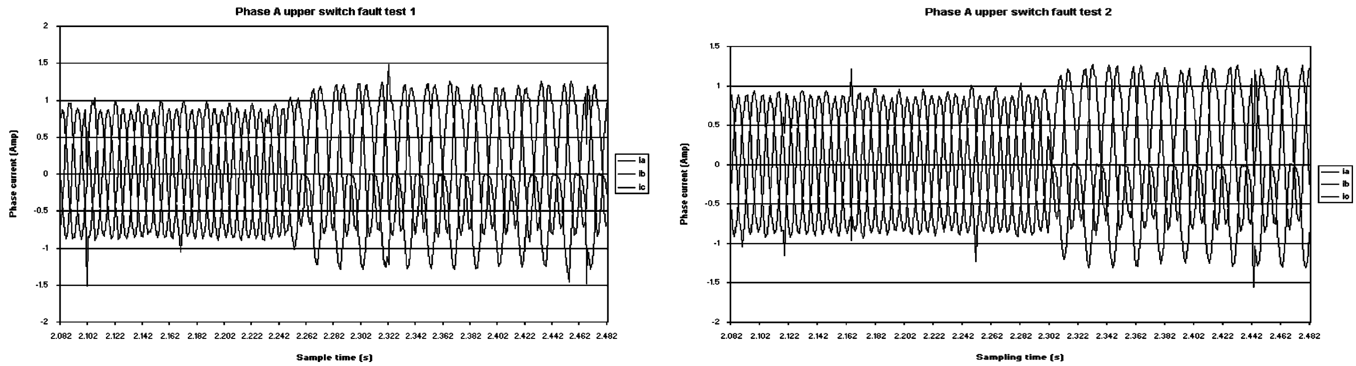

Fig. 17. $I_\mathrm{a}, I_\mathrm{b}$, and I_c signals generated at two separate occasions with switch A broken.

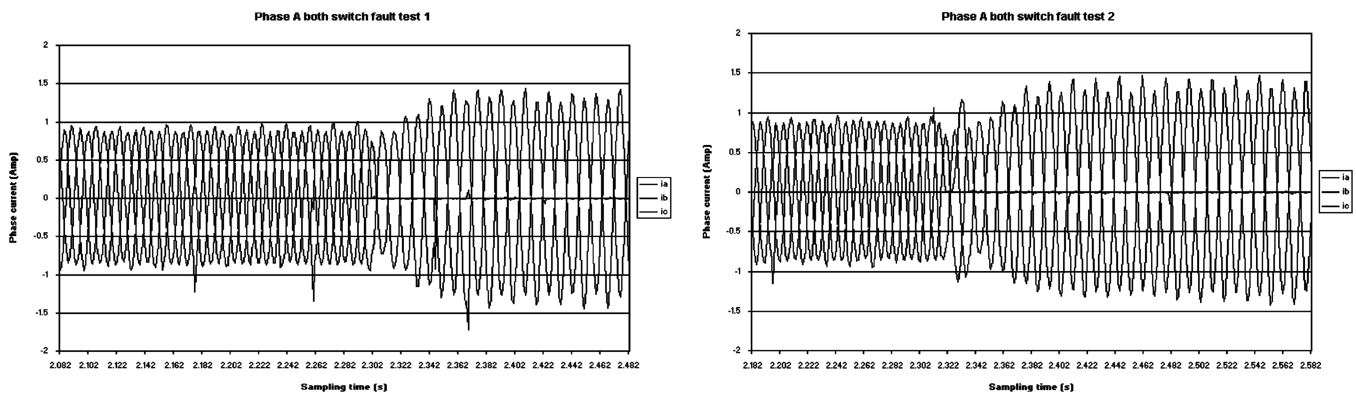

Fig. 18. $I_\mathrm{a}, I_\mathrm{b}$, and I_c generated by the bench setup circuit system with switches A and A′ broken.

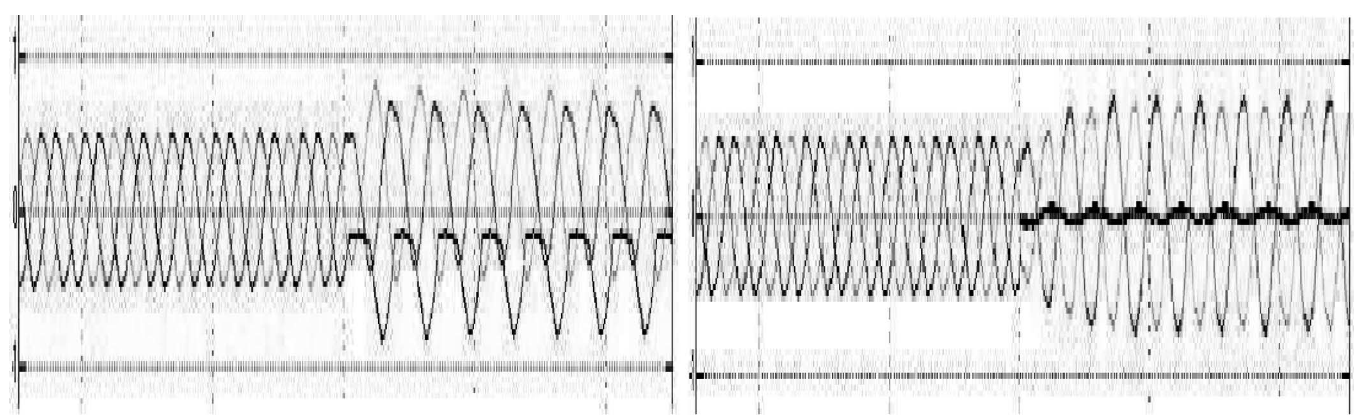

(a) (b)

Fig. 19. Current signals generated by SIM_drive with switch A broken and both A and A′ broken. (a) $I_\mathrm{a}, I_\mathrm{b}$, and I_c signals generated by the simulated model with switch A broken. (b) $I_\mathrm{a}, I_\mathrm{b}$, and I_c signals generated by the circuit system with switches A and A′ broken.

control and a sine-triangle PWM method for synthesizing reference voltage command generated by the FOC.

A machine learning algorithm, CP-Select, was designed to select the representative operating conditions in terms of torque and speed such that the signals generated by SIM_drive at these operating points can be used to train a robust diagnostic system. The CP-Select uses a novel procedure "select-simulation-evaluation" that systematically selects the torque-speed operating points for training, and generates signals at the selected points and evaluates the system trained at these points, and CP-Select stops when the system performance is satisfactory. We presented two neural network architectures, a structured multi-neural-network system, and a single-neural-network system. The structured multi-neural-network system showed superior performance, whereas the single-neural-network system is easier to implement and train.

The proposed model-based diagnostic system trained with the machine learning technology has been evaluated by two sets of experiments. In the first set of experiments, we used the test signals generated by the SIM_drive that contain the

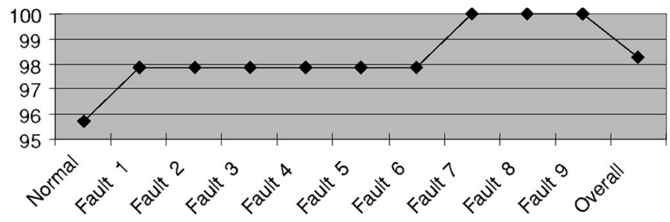

Fig. 20. Performance of a model-based fault diagnostic system on data generated by experimental bench setup system.

normal and nine faulty classes. In the second set of experiments, we used the data generated by a bench setup in the laboratory to test the model-based fault diagnostic system trained on the signals generated by the simulated electric drive. The model-based fault diagnostic system performed very well in both sets of data. We are particularly encouraged by the results obtained on the data generated by the bench setup, where the model-based fault diagnostic system prediction accuracies were close to 98% or above in detecting nine classes of faults: Six single-switch broken classes and three post-short-circuit fault classes.

In conclusion, the proposed model-based fault diagnostics approach is found to be very effective in detecting multiple classes of faults in an electric drive inverter. The authors would like to point out that the training phase in the proposed approach is elaborate to make the resulting diagnostic system accurate and robust. However, once the training is complete, the implementation in a diagnostic system is quite simple, since thereafter, the weights of the resulting diagnostic neural network can be stored in and processed by a fast and low-cost processor. A significant contribution of this work is the presentation of a generalized methodology for developing fault diagnostics systems: a technically sound simulated system model combined with machine learning techniques to train a robust diagnostic system, which can be applied to a broad range of applications including real-time systems.

Acknowledgment

The authors would like to thank Prof. C. Mi and graduate student H. Wu at the ECE Department, University of Michigan-Dearborn, Dearborn, for building the three-phase induction motor setup in the laboratory and performing many experiments to generate the data needed for validating the work presented in this paper.

References

[1] C. C. Chan and K. T. Chau, *Modern Electric Vehicle Technology*. London, U.K.: Oxford Univ. Press, 2001.

[2] R. Hodkinson and J. Fenton, *Lightweight Electric/Hybrid Vehicle Design*. Warrendale, PA: SAE, 2001.

[3] D. W. Novotny and T. A. Lipo, *Vector Control and Dynamics of AC Drives*. Oxford, U.K.: Oxford Science, 1996.

[4] A. Bakhshai, G. Joos, J. Espinoza, and H. Jin, "Fast space vector modulation based on a neurocomputing digital signal processor," in *Proc. Applied Power Electronics Conf. Expo.*, 1997, vol. 12, pp. 872–878.

[5] N. Mohan, T. Undeland, and W. Robbins, *Power Electronics*. New York: Wiley, 1995.

[6] Y. Kao and C. Liu, "Analysis and design of microprocessor-based vector-controlled induction motor drives," *IEEE Trans. Ind. Electron.*, vol. 39, no. 1, pp. 46–54, Feb. 1992.

[7] C. Liaw, K. Chao, and F. Lin, "A discrete adaptive field-oriented induction motor drive," *IEEE Trans. Power Electron.*, vol. 7, no. 2, pp. 411–419, Apr. 1992.

[8] J. Holtz, "Pulse width modulation—A survey," *IEEE Trans. Ind. Electron.*, vol. 39, no. 5, pp. 411–420, Dec. 1992.

[9] M. A. Masrur, X. Xu, and F. Liang, "Fault isolation in an induction motor control system," U.S. Patent 5469351, Nov. 1995.

[10] J. Klima, "Analytical investigation of an induction motor drive under inverter fault mode operations," *IEE Proc.- Electr. Power Appl*, vol. 150, no. 3, pp. 255–262, May 2003.

[11] J. Gertler, M. Costin, X. Fang, Z. Kowalczuk, M. Kunwer, and R. Monajemy, "Model based diagnosis for automotive engines-algorithm development and testing on a production vehicle," *IEEE Trans. Contr. Syst. Technol.*, vol. 3, no. 1, pp. 61–69, Mar. 1995.

[12] M. Nyberg, "Model-based diagnosis of an automotive engine using several types of fault models," *IEEE Trans. Contr. Syst. Technol.*, vol. 10, no. 5, pp. 679–689, Sep. 2002.

[13] Y. L. Murphey, H. Guo, J. A. Crossman, and M. Coleman, "Automotive signal diagnostics using wavelets and machine learning," *IEEE Trans. Veh.*, vol. 49, no. 5, pp. 1650–1662, Sep. 2000.

[14] J. A. Crossman, H. Guo, Y. L. Murphey, and J. Cardillo, "Automotive signal fault diagnostics—Part I: Signal fault analysis, feature extraction, and quasi optimal signal selection," *IEEE Trans. Veh.*, vol. 52, no. 4, pp. 1063–1075, Jul. 2003.

[15] Y. L. Murphey, J. A. Crossman, Z. Chen, and J. Cardillo, "Automotive fault diagnosis, Part II: A distributed agent diagnostic system," *IEEE Trans. Veh.*, vol. 52, no. 4, pp. 1076–1098, Jul. 2003.

[16] O. Moseler and R. Isermann, "Application of model-based fault detection to a brushless DC motor," *IEEE Trans. Ind. Electron.*, vol. 47, no. 5, pp. 1015–1020, Oct. 2000.

[17] R. Ribeiro, C. B. Jacobina, and E. Silva, "Fault detection of open-switch damage in voltage-fed PWM motor drive system," *IEEE Trans. Power Electron.*, vol. 18, no. 2, pp. 587–593, Mar. 2003.

[18] W. Fenton, T. McGinnity, and L. Maguire, "Fault diagnosis of electronic systems using intelligent techniques: A review," *IEEE Trans. Syst., Man, Cybern. C*, vol. 31, no. 3, pp. 269–281, Aug. 2000.

[19] K. Kim and A. G. Parlos, "Induction motor fault diagnosis based on neuropredictors and wavelet signal processing," *IEEE/ASME Trans. Mechatronics*, vol. 7, no. 2, pp. 201–219, Jun. 2002.

[20] F. Filippetti, G. Franceschini, C. Tassoni, and P. Vas, "Recent developments of induction motor drives fault diagnosis using AI techniques," *IEEE Trans. Ind. Electron.*, vol. 47, no. 5, pp. 994–1004, Oct. 2000.

[21] F. Zidani, M. Benbouzid, D. Diallo, and M. Said, "Induction motor stator faults diagnosis by a current concordia pattern-based fuzzy decision system," *IEEE Trans. Energy Convers.*, vol. 18, no. 4, pp. 469–475, Dec. 2000.

[22] M. Benbouzid, "Bibliography on induction motor faults detection and diagnosis," *IEEE Trans. Energy Convers.*, vol. 14, no. 4, pp. 1065–1074, Dec. 1999.

[23] M. Chow, *Methodologies of Using Neural Network and Fuzzy Logic Technologies for Motor Incipient Fault Detection*. Singapore: World Scientific, 1997.

[24] D. Kastha and B. Bose, "Investigation of fault modes of voltage-fed inverter system for induction motor drive," *IEEE Trans. Ind. Appl.*, vol. 30, no. 4, pp. 1028–1038, Jul.–Aug. 1994.

[25] K. Smith, L. Ran, and J. Penman, "Real-time detection of intermittent misfiring in a voltage-fed PWM inverter induction-motor drive," *IEEE Trans. Ind. Electron.*, vol. 44, no. 4, pp. 468–476, Aug. 1997.

[26] Y. LeCun, L. Bottou, Y. Bengio, and P. Haffner, "Gradient-based learning applied to document recognition," *Proc. IEEE*, vol. 86, no. 11, pp. 2278–2324, Nov. 1998.

[27] L. A. Feldkamp and G. V. Puskorius, "A signal processing framework based on dynamic neural networks with application to problems in adaptation, filtering, and classification," *Proc. IEEE*, vol. 86, no. 11, pp. 2259–2277, Nov. 1998.

[28] K. Fukushima, "A neural network for visual pattern recognition," *IEEE Comput.*, vol. 21, no. 3, pp. 65–75, Mar. 1998.

[29] L. Zhao and E. Thorpe, "Stereo- and neural network-based pedestrian detection," *IEEE Trans. Intell. Transp. Syst.*, vol. 1, no. 3, pp. 148–154, Sep. 2000.

[30] W. Y. Huang and R. P. Lippmann, *Neural net and traditional classifiers* in *Neural Information Processing Systems*, D. Z. Anderson, Ed. New York: American Institute of Physics, pp. 387–396, 1988.

[31] E. L. Allwein and R. E. Schapire, "Reducing multiclass to binary: A unifying approach for margin classifiers," *J. Mach. Learning Res.*, vol. 1, pp. 113–141, 2000.
[32] D. Price, S. Knerr, L. Personnaz, and G. Dreyfus, "Pairwise neural network classifiers with probabilistic outputs," in *Advances in Neural Information Processing Systems 7 (NIPS-94)*, G. Tesauro, D. Touretzky, and T. Leen, Eds. Cambridge, MA: MIT Press, 1995, vol. 7, pp. 1109–1116.
[33] S. Har-Peled, D. Roth, and D. Zimak, "Constraint classification: A new approach to multiclass classification," in *Proc. 13th Int. Conf. Algorithmic Learning Theory*, 2002, pp. 365–397.
[34] X. Li, X.-C. Yao, Y. L. Murphey, R. Karlsen, and G. Gerhart, "A real-time vehicle detection and tracking ststem in outdoor traffic scenes," in *Proc. Int. Conf. Pattern Recognit.*, Cambridge, U.K., 2004, vol. 2, pp. 761–764.
[35] G. Ou, Y. L. Murphey, and L. Feldkamp, "Multiclass pattern classification using neural networks," presented at the Int. Conf. Pattern Recognition, Cambridge, UK, 2004.
[36] Y. L. Murphey, Z.-H. Chen, and L. Feldkamp, "Incremental neural learning using AdaBoost," in *Proc. IEEE Int. Joint Conf. Neural Netw.*, 2002, vol. 3, pp. 2304–2308.

Yi Lu Murphey (S'85–M'88–SM'97) received the M.S. degree in computer science from Wayne State University, Detroit, MI, in 1983 and the Ph.D. degree in computer, information, and control engineering from the University of Michigan, Ann Arbor, in 1989.

She was a Research Scientist at the Environmental Research Institute of Michigan, Ann Arbor. Since 1992, she has been a Professor of electrical and computer engineering at the University of Michigan-Dearborn, Dearborn. Her recent research projects include fault diagnostics, distributed agent systems, computer vision systems for robotic vehicles, incremental learning in neural networks, support vector machine learning from large data sets, hybrid learning system with neural networks and genetic algorithms, data mining from text documents, and data mining from time-series data. Her research interests include machine learning, computer vision, and intelligent systems.

M. Abul Masrur (M'84–SM'93) received the Ph.D. degree in electrical engineering from Texas A&M University, College Station, in 1984.

From 1984 to 2001, he was with the Scientific Research Laboratories, Ford Motor Company, and was involved in research and development related to simulation and control for electric drives for electric and hybrid electric vehicles and power electronics, advanced automotive electric energy management and vehicular power system architecture, automotive multiplexing systems, and related works. In 2001, he joined the Vetronics Technology Department, U.S. Army RDECOM-TARDEC, Warren, MI, where he is involved in various vehicular electric power system architecture concept design and development for military applications. He has over 50 publications and holds 8 U.S. patents.

Dr. Masrur has been an Associate Editor of the IEEE TRANSACTIONS ON VEHICULAR TECHNOLOGY since 1999. He received the Best Automotive Electronics Paper Award from the IEEE Vehicular Technology Society, USA, in 1998.

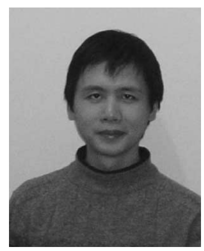

ZhiHang Chen received the Ph.D. degree in applied mathematics from Peking University, Beijing, China, in 2000.

Currently, he is a Research Associate at the University of Michigan-Dearborn, Dearborn. His research interests include machine learning, intelligence system, neural networks, genetic algorithms, and fuzzy logic.

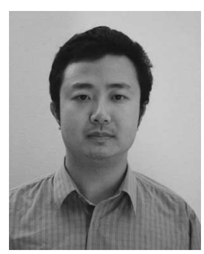

Baifang Zhang received the B.S. degree in computer science from East Normal University, Shanghai, China, in 1998. He is currently pursuing a Master of Engineering program in computer engineering at the University of Michigan-Dearborn, Dearborn.

From 1998 to 2002, he was with Panaelectronics Inc. His research interests include signal/time series analysis using artificial intelligent methods, vehicle fault diagnosis, and vehicle control systems.